A cylindrical δ-potential in external magnetic fields: a model for semiconductor nanostructures

1996 J. Phys.: Condens. Matter 8 2197

(http://iopscience.iop.org/0953-8984/8/13/011)

J. Phys.: Condens. Matter **8** (1996) 2197–2208. Printed in the UK

A cylindrical δ-potential in external magnetic fields: a model for semiconductor nanostructures

Oleg Olendski and Chang Sub Kim

Department of Physics, Chonnam National University, Kwangju 500-757, Korea

Received 5 January 1996

Abstract. A semiconductor nanostructure represented by the cylindrical electrostatic δ-potential subjected to magnetic fields is considered theoretically. The possibility of particle penetration into the region outside the ring for a finite opacity leads to modification of the energy spectrum and the associated azimuthal currents compared to the results for the quantum ring. In particular, when the Aharonov–Bohm whisker is introduced at the origin the currents do not tend to zero in the limit of vanishing magnetic flux. This is attributed to the change of the topology of the structure after introducing the non-zero Aharonov–Bohm flux. This feature diminishes when more realistic distributions of the magnetic field are considered. For uniform magnetic fields anticrossings of the energy levels are observed as a function of the magnetic index and their role in determining the quantum currents is investigated for a wide range of the potential strength. Similarities and differences between the rectangular and cylindrical geometry are discussed.

The concept of the δ-potential provides the simplest and most convenient mathematical description of physical phenomena. For instance, it finds a wide application in miscellaneous theoretical models [1]. Recently, the problem of a one-dimensional δ-potential in an external magnetic field was considered theoretically in an attempt to model a simple semiconductor microstructure [2]. A comparison with finite rectangular barriers [3, 4] or a well [5] reveals that the δ-potential model studied correctly captures the main characteristics of more realistic structures. In this work the energy spectrum and the associated azimuthal currents are investigated for a model quantum structure represented by a cylindrical δ-potential of strength Ω subjected to various configurations of applied magnetic fields. The situations considered are:

(1) Aharonov–Bohm flux [6, 7] threading at the origin;
(2) a uniform magnetic field in the interior of the ring directed along the symmetric axis and zero outside;
(3) a uniform axial magnetic field over all of the space.

The motivation for the present investigation is that similar structures with cylindrical symmetry have attracted a lot of theoretical [8, 13] and experimental [14, 16] attention in connection with the problem of persistent currents [17]. The most obvious difference between previous studies and the model proposed here is the fact that the former studies consider electrons *rigidly* bounded on the ring while for our model with $\Omega < 0$ there is a non-zero probability of particle penetration into the region outside the ring. Therefore, the radial part of the wavefunction becomes an important factor in determination of the eigenenergies and eigenstates. In the limit of $\Omega \to -\infty$ we recover the previous results for rigidly

0953-8984/96/132197+12$19.50

bounded electrons. However, in the intermediate regime predictions of the two models are different. Throughout our calculations we assume a ballistic regime of electron motion, i.e., the mean free path of an electron is assumed to be much larger than the perimeter of the ring $L_p = 2\pi\rho_p$, with ρ_p being the radius of the ring. Also, since recently it was shown theoretically that the effect of electron–electron interaction on persistent currents may be neglected [18, 19], we adopt an independent-electron picture with a single effective mass.

Let us start by considering the configuration of the cylindrical δ-potential of radius ρ_p, circumference $L_p = 2\pi\rho_p$, and strength $(\hbar^2/m_e^*)\Omega$:

$$V(\rho) = \frac{\hbar^2}{m_e^*}\Omega\,\delta\big(\rho - \rho_p\big) \tag{1}$$

where m_e^* is the effective mass of the electron. Positive opacity of the potential $\Omega > 0$ corresponds to the repulsive potential and negative opacity ($\Omega < 0$) to the attractive one. We introduce also the Aharonov–Bohm flux Φ pierced along the axis of symmetry of the ring potential. The relevant single-particle equation is written in plane polar coordinates $\boldsymbol{r} = (\rho, \varphi)$ as ($c \equiv 1$)

$$\left\{\frac{1}{2m_e^*}\,(\boldsymbol{p} + e\boldsymbol{A})^2 + V(\rho)\right\}\Psi(\rho,\varphi) = E\Psi(\rho,\varphi) \tag{2}$$

where e is the absolute charge of an electron and $\boldsymbol{A}$ is the vector potential. In the symmetric gauge adopted here only the tangential component of the vector potential is not zero:

$$A_\varphi = \frac{\Phi}{2\pi\rho}.$$

Then, one can separate out variables by making use of the *ansatz*

$$\Psi(\rho,\varphi) = \frac{1}{\sqrt{2\pi}}R(\rho)\exp(\mathrm{i}m\varphi) \tag{3}$$

where m is the magnetic quantum number and the radial wavefunction is subjected to

$$\frac{\mathrm{d}^2}{\mathrm{d}\rho^2}R + \frac{1}{\rho}\frac{\mathrm{d}}{\mathrm{d}\rho}R - \left(\frac{2m_e^*|E|}{\hbar^2} + \frac{(m+\phi)^2}{\rho^2}\right)R - 2\Omega\,\delta\big(\rho - \rho_p\big)\,R = 0. \tag{4}$$

Since bound states can exist only for $E < 0$, we have explicitly incorporated this into equation (4) where the absolute value of energy is present. Also, in equation (4) ϕ is defined to be

$$\phi = \frac{\Phi}{\Phi_0} \tag{5}$$

with $\Phi_0 = h/e$ being a flux quantum. Since all properties of the system are periodic in Φ with a period Φ_0 and possess definite symmetry with respect to $\phi = 0$, only the case $0 \leqslant \phi \leqslant 0.5$ is considered below.

Solutions to equation (4) are

$$R(\rho) = A_- I_{|m+\phi|}\left(\frac{1}{\hbar}\sqrt{2m_e^*|E|}\rho\right) \qquad \rho < \rho_p \tag{6}$$

$$R(\rho) = A_+ K_{|m+\phi|}\left(\frac{1}{\hbar}\sqrt{2m_e^*|E|}\rho\right) \qquad \rho > \rho_p \tag{7}$$

where $I_\nu(x)$ and $K_\nu(x)$ are the modified Bessel functions [20] and $A_\pm$ are the normalization constants. Using the same arguments as in the case of the one-dimensional δ-potential [21], one can readily derive matching conditions for the cylindrical δ-potential:

$$R\big(\rho_p - 0\big) = R\big(\rho_p + 0\big) \tag{8}$$

$$\frac{\mathrm{d}}{\mathrm{d}\rho}R(\rho_p+0)-\frac{\mathrm{d}}{\mathrm{d}\rho}R(\rho_p-0)=2\Omega R(\rho_p)\,. \tag{9}$$

Applying these to the configurations discussed and after some algebra, one can obtain

$$\left|\Omega^*\right| I_{|m+\phi|}\left(\left|E^*\right|^{1/2}\right) K_{|m+\phi|}\left(\left|E^*\right|^{1/2}\right)=1 \tag{10}$$

which determines the energy eigenvalues. In the above the following normalized quantities have been introduced:

$$\Omega^*=2\Omega\rho_p \qquad \text{and} \qquad E^*=E\Big/\left(\frac{\hbar^2}{2m_e^*\rho_p^2}\right) \tag{11}$$

and also use has been made of the fact that bound states can exist only for negative Ω^*.

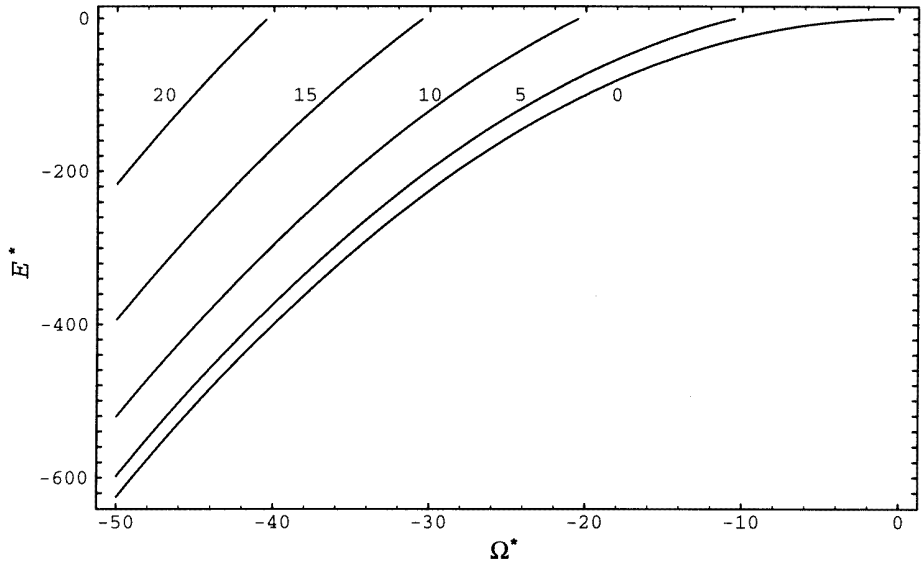

Figure 1. The energy spectrum E^* as a function of the potential strength Ω^* for $\phi=0.2$; numbers near the curves denote the quantum number m.

This result deserves some attention. First, equation (10) gives rise to a finite number of bound states for a finite negative Ω^* unlike the one-dimensional δ-potential because of the additional degree of freedom along the azimuthal direction. Also, it follows from the asymptotic properties of the modified Bessel functions for small argument [20] that there appears a threshold value of $|\Omega^*|$ that triggers a new bound state: the energy level with a particular quantum number m can exist only when $|\Omega^*|$ is bigger than $2|m+\phi|$. In particular, for $\phi=0$ at least one bound level exists regardless of $|\Omega^*|$. However, if the well is shallow, introducing an Aharonov–Bohm whisker can convert this level into an unbound state. In the opposite limit of very deep wells, the normalized energies depend on Ω^* quadratically:

$$\left|E^*\right|\approx\frac{1}{4}\left|\Omega^*\right|^2. \tag{12}$$

These features of the energy spectrum are shown in figure 1 where E^* is plotted as a function of Ω^* for several m with $\phi=0.2$. Here, it should be noticed that the radial quantum number has been suppressed due to the delta potential, and accordingly only the

magnetic quantum number appears. It is seen that the level with $m = 0$ always has the least energy as compared to other levels. This level exists for all values of $\Omega^* \leqslant -2|\phi|$. For very shallow wells, i.e. when $\Omega^* \simeq -2|\phi|$, it is located near the top of the δ-potential: $|E^*| \approx 0$. Figure 1 clearly manifests that there exist the aforementioned threshold values of $|\Omega^*| = 2|m + \phi|$. In the opposite limit of $\Omega^* \to -\infty$ we come to the system of electrons rigidly bounded on the quantum ring studied in [8].

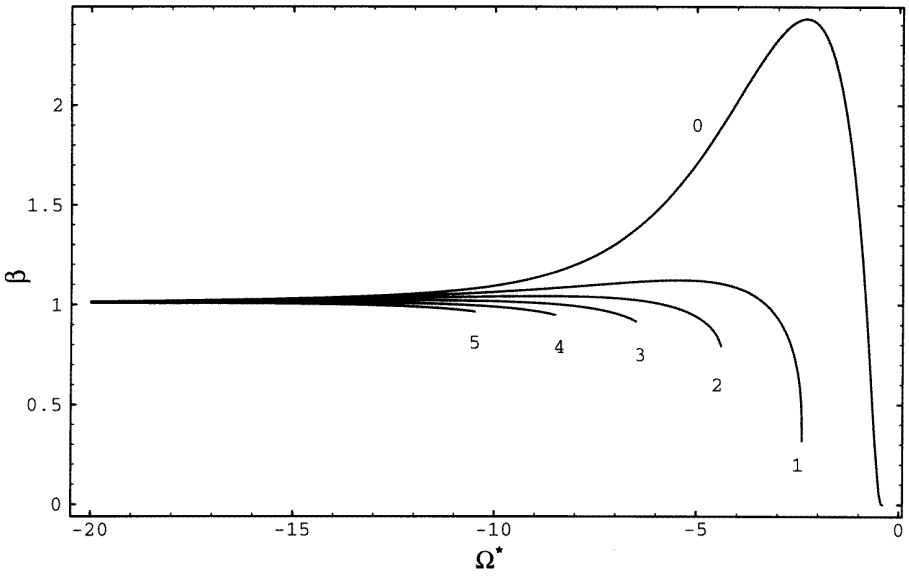

Figure 2. The value β as a function of Ω^* for several levels; numbers near the curves denote the quantum number m.

The correspondence between our proposed model and the structure studied in [8] becomes more evident if one computes the associated currents. In the present investigation only the azimuthal component is relevant and it can be obtained by integrating the following current density over the radial axis [22]:

$$j_\varphi(\rho) = -\frac{1}{2\pi}\frac{e\bar{h}}{m_e^*}\left[\frac{m}{\rho} + \frac{e}{\bar{h}}A_\varphi(\rho)\right]R^2(\rho). \tag{13}$$

The current J carried by the state with a definite quantum number m is given as

$$J = -\frac{2\pi e\bar{h}}{m_e^* L_p^2}(m + \phi)\,\beta \tag{14}$$

where a normalization condition has been used:

$$\int_0^\infty R^2(\rho)\rho\ \mathrm{d}\rho = 1.$$

Comparing this with the case of electrons rigidly bounded on the ring, equation (2.2) in [8], one sees that the only difference is the appearance of the term

$$\beta = \left|E^*\right|\left(\int_0^{|E^*|^{1/2}} I^2_{|m+\phi|}(\rho)\frac{\mathrm{d}\rho}{\rho} + \gamma^2\int_{|E^*|^{1/2}}^\infty K^2_{|m+\phi|}(\rho)\frac{\mathrm{d}\rho}{\rho}\right)$$

$$\times\left(\int_0^{|E^*|^{1/2}} I^2_{|m+\phi|}(\rho)\rho\ \mathrm{d}\rho + \gamma^2\int_{|E^*|^{1/2}}^{\infty} K^2_{|m+\phi|}(\rho)\rho\ \mathrm{d}\rho\right)^{-1} \tag{15}$$

where

$$\gamma = \frac{I_{|m+\phi|}\left(|E^*|^{1/2}\right)}{K_{|m+\phi|}\left(|E^*|^{1/2}\right)}. \tag{16}$$

This term appears because we take into account the possibility of particle penetration into the region outside the ring. The quantity β is shown in figure 2 as a function of Ω^* for $\phi = 0.2$. It is shown that for increasing $|\Omega^*|$ the results rapidly approach those for an infinite δ-potential: $\beta \to 1$. It is also manifested that for levels with $|m| \geqslant 3$ the value of β is very close to unity even at the threshold values of Ω^*. Since the largest deviations from the results for the infinite well occur at the level with $m = 0$, we will concentrate on it in the following. It is shown that as $\Omega^* \to -2\,|\phi|$ the current for $m = 0$ tends to zero. The value of β increases first while the depth of the well gets bigger, and after passing through a maximum it decreases gradually to unity.

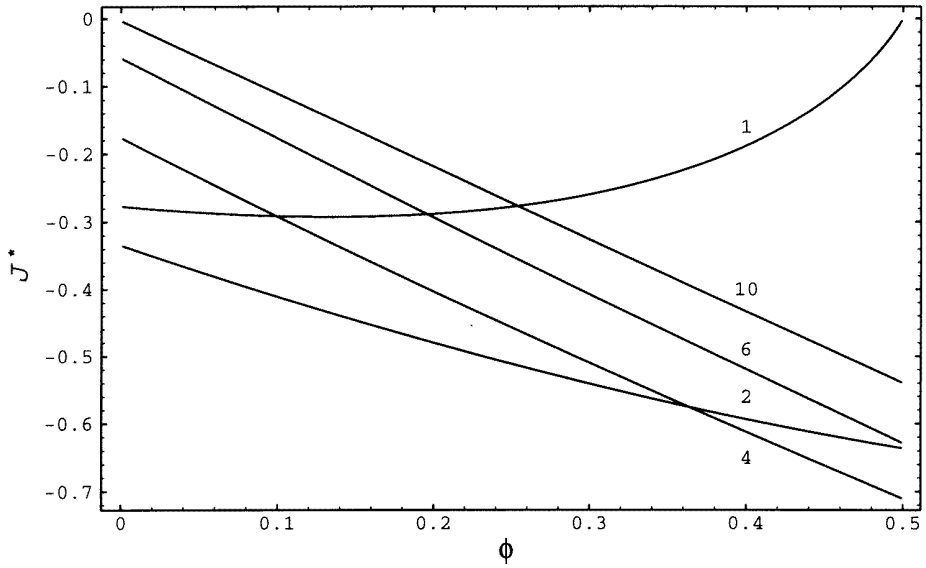

Figure 3. The current J^* carried by the level $m = 0$ versus the normalized Aharonov–Bohm flux ϕ for several Ω^*; numbers near the curves denote the value of $|\Omega^*|$.

Next, the J–ϕ characteristic curves for the level of $m = 0$ are plotted in figure 3 for varying depth of the ring potential, where the normalized current J^* is used:

$$J^* = J\Big/\left(\frac{2\pi e\bar{h}}{m_e^* L_p^2}\right). \tag{17}$$

This shows that at small $|\Omega^*|$ the dependence of the current on the flux is not linear. The prominent feature of the J–ϕ characteristic curves that we obtained is that the current is not a continuous function of the flux at $\phi = 0$; in fact, it is seen that current, which is zero identically at $\phi = 0$ (see equation (14)), has a non-vanishing value at any infinitesimally small ϕ. This is due to the fact that introduction of the Aharonov–Bohm whisker at the origin changes the topology of the system considered. As a result, the wavefunction for

$m = 0$, which is non-zero at $\rho = 0$ without the Aharonov–Bohm flux, should vanish at the origin when $\phi \neq 0$. This also explains why the largest deviation takes place for the state with $m = 0$ in figure 2 since even in the absence of the flux the wavefunctions with non-zero m vanish at $\rho = 0$. Also, it is observed that the discontinuous jump of the currents becomes smaller on increase of $|\Omega^*|$. This is because for the deeper wells the value of the wavefunction at the origin is smaller in the absence of the magnetic whisker, and accordingly introduction of the central flux does not alter the behaviour of the wavefunction at the origin significantly. And, for $|\Omega^*| = 10$ we almost recover the continuous and linear dependence of the J–ϕ characteristic of the infinite δ-potential.

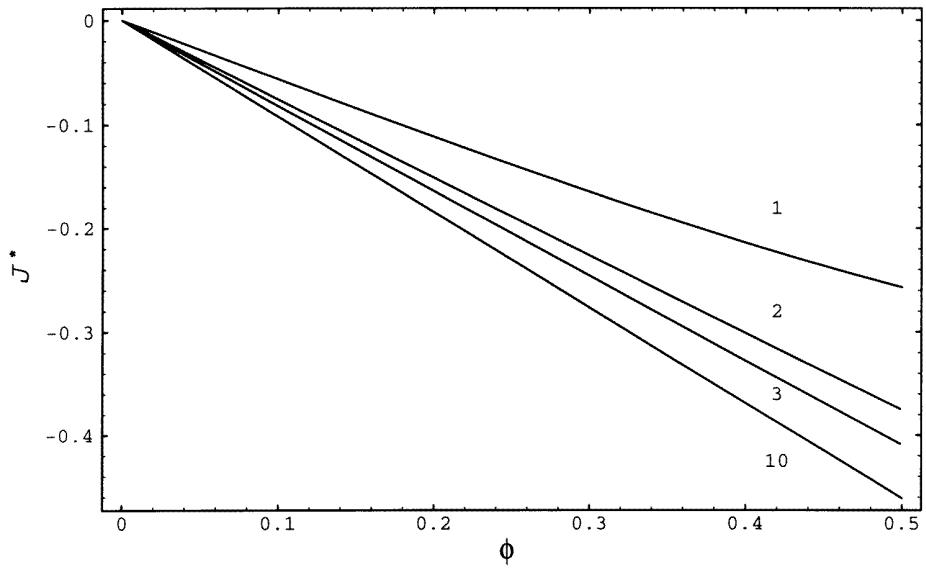

Figure 4. As figure 3, but for the structure with magnetic fields uniform inside the ring but zero outside; numbers near the curves denote the value of $|\Omega^*|$.

In order to eliminate the above-mentioned discontinuity in the J–ϕ characteristic, one must deal with more realistic distributions of the magnetic field. To demonstrate this we have performed calculations for the ring structure with a magnetic field $\boldsymbol{B} = (0, 0, B)$ which is applied uniformly inside the region of the ring and zero outside, where the ring lies in the xy-plane:

$$B(\rho) = \begin{cases} B & \rho \leqslant \rho_p \\ 0 & \rho > \rho_p. \end{cases} \tag{18}$$

The Aharonov–Bohm whisker has been removed from the centre in the present structure. Non-uniform configurations of the magnetic field have become of increasing theoretical interest [23, 24] due to the progress in the growth technology [25–27]. For the magnetic field given by equation (18) the most convenient choice of the vector potential is as follows:

$$A_\varphi(\rho) = \begin{cases} \dfrac{1}{2} B\rho & \rho \leqslant \rho_p \\ \dfrac{1}{2} \dfrac{B\rho_p^2}{\rho} & \rho > \rho_p. \end{cases} \tag{19}$$

By varying the magnetic field B one changes the total magnetic flux $\Phi = \pi B\rho_p^2$. Outside the ring the electron wavefunction is still described by equation (7). On the other hand, inside the ring the solution of the Schrödinger equation reads now

$$R(\rho) = A_- \exp\left(-\frac{1}{4}\frac{\rho^2}{r_B^2}\right)\left(\frac{1}{2}\frac{\rho^2}{r_B^2}\right)^{|m|/2} \times M\left(\frac{1+m+|m|}{2} - \frac{E}{\hbar\omega_B}, |m|+1, \frac{1}{2}\frac{\rho^2}{r_B^2}\right) \qquad \rho < \rho_p. \tag{20}$$

In the above $M(a,b,x)$ is the confluent hypergeometric function [20], $\omega_B = eB/m_e^*$ is the cyclotron frequency, and $r_B = \sqrt{\hbar/eB}$ is the magnetic radius. Applying magnetic fields in the region $\rho \leqslant \rho_p$ does not lift the suppression of radial quantum number and thus only the magnetic quantum number is present. The form of the wavefunction suggests that it remains finite at $\rho = 0$ for $m = 0$ with non-zero flux. Consequently, the current is a continuous function of the flux at $\phi = 0$ as is clearly seen in figure 4 where the J–ϕ characteristics are plotted for the present configuration for $m = 0$. It should be noticed that in the present configuration, contrary to the case of Aharonov–Bohm flux, the magnitude of the current is always smaller as compared to the result for infinite opacity. Increasing $|\Omega^*|$ causes the slope of the J–ϕ characteristic to increase and eventually to approach the previously known results in the limit of $\Omega^* \to -\infty$ [8].

As the third configuration we shall discuss the problem of a δ-potential in uniform magnetic fields. In this case the radial part of the wavefunction for $\rho < \rho_p$ is described by equation (20), and outside the ring it is given as

$$R(\rho) = A_+ \exp\left(-\frac{1}{4}\frac{\rho^2}{r_B^2}\right)\left(\frac{1}{2}\frac{\rho^2}{r_B^2}\right)^{|m|/2} \times U\left(\frac{1+m+|m|}{2} - \frac{E}{\hbar\omega_B}, |m|+1, \frac{1}{2}\frac{\rho^2}{r_B^2}\right) \qquad \rho > \rho_p \tag{21}$$

where the special function $U(a,b,x)$ is an another solution to Kummer's equation, which is linearly independent of $M(a,b,x)$ [20]. The matching procedure using equations (8) and (9) produces the transcendental equation for determination of the energy spectrum:

$$M\left(\frac{1+m+|m|}{2} - E^*, |m|+1, \frac{1}{2}r_p^2\right)U\left(\frac{1+m+|m|}{2} - E^*, |m|+1, \frac{1}{2}r_p^2\right) = -\frac{2^{|m|+1}}{\Omega^*}\frac{(|m|)!\exp\left(\frac{1}{2}r_p^2\right)}{r_p^{2|m|}\Gamma\left((1+m+|m|)/2 - E^*\right)} \tag{22}$$

where $\Gamma(x)$ is the Gamma function and the variables are normalized according to

$$E^* = \frac{E}{\hbar\omega_B} \qquad r_p = \frac{\rho_p}{r_B}. \tag{23}$$

In this case the energy eigenvalues are specified by two quantum numbers, the radial quantum number n and magnetic quantum number m, unlike in the previous two situations.

A few asymptotic cases can be deduced from equation (22). First, at $\Omega^* = 0$ one gets the usual Landau levels of the form

$$E^* = n + \frac{1}{2}\left(|m| + m + 1\right). \tag{24}$$

In the case of vanishing magnetic field, using the properties of the confluent hypergeometric functions [20], one recovers equation (10) with $\phi = 0$. Also, the limit $|\Omega^*| \to \infty$ in equation (22) leads to the condition

$$M\left(\frac{1+m+|m|}{2} - E^*, |m|+1, \frac{1}{2}r_p^2\right)U\left(\frac{1+m+|m|}{2} - E^*, |m|+1, \frac{1}{2}r_p^2\right) = 0. \qquad (25)$$

When the delta potential is repulsive, equation (25) results in either an electron confined in a quantum disk of radius ρ_p (when the function M is equal to zero) or an electron located outside the disk (when the function $U(a, b, x)$ is zero). In particular, the former situation was treated in detail in [11, 28]. On the other hand, when the delta potential is attractive, equation (25) corresponds to the problem of the quantum ring that was considered in [8].

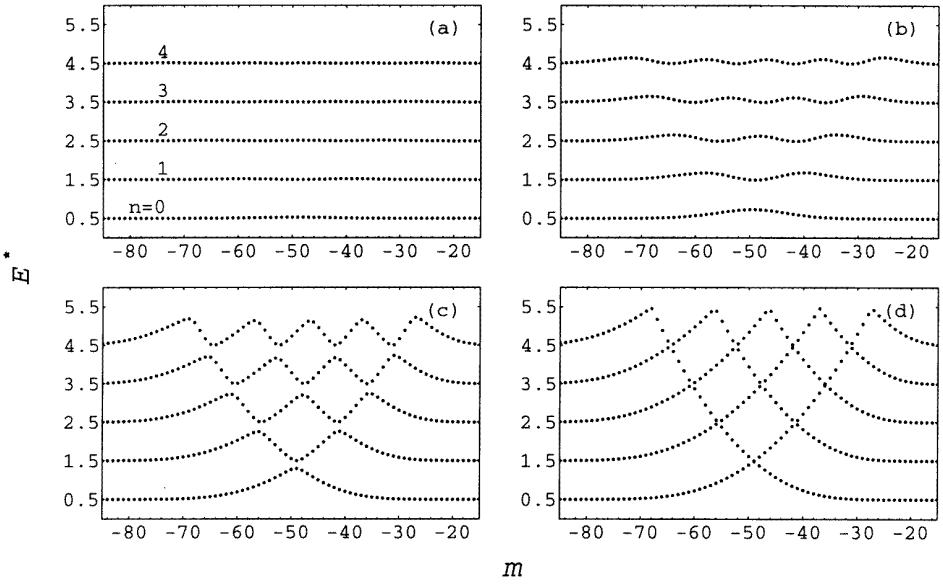

Figure 5. Energy dispersion relations for the structure with uniform magnetic fields in terms of magnetic index m for $r_p = 10$ and (a) $\Omega^* = 1$, (b) $\Omega^* = 10$, (c) $\Omega^* = 100$, and (d) $\Omega^* = 1000$; numbers near the curves denote the quantum number n.

The outcome of calculations of equation (22) for general soft δ-potentials are presented here. The energy spectra E^* for several positive and negative Ω^* are shown in terms of the magnetic index m for several radial quantum numbers n in figure 5 and figure 6 respectively. They manifest a similar behaviour to the corresponding case of the one-dimensional δ-potential on replacing the centre of magnetic oscillations y_0 by the magnetic index m [2]. Introducing the electrostatic potential into the uniform magnetic field induces a lift of the degeneracy of the Landau levels. At small $|\Omega^*|$ it is seen that the deviation of the energies from the Landau levels is small on varying the magnetic index m. In this case it is difficult to speak of any interaction between levels with different principal quantum numbers n. Increasing $|\Omega^*|$ disturbs magnetic states more strongly and consequently the levels with adjacent n get closer to each other at some values of m. Going from parts (a) to (d) in figures 5 and 6, one clearly sees how the anticrossings and repulsions of levels are built up in the energy spectrum on increase of $|\Omega^*|$. It is worthwhile to note that for a positive (negative) Ω^* every nth level ($n = 0, 1, 2, \ldots$) has $n + 1$ maxima (minima) in figure 5

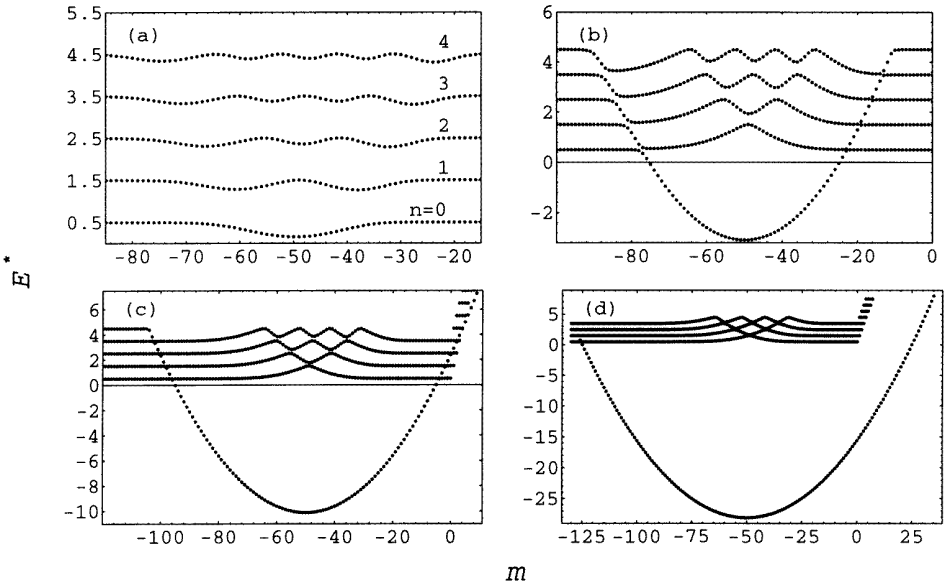

Figure 6. As figure 5, but for attractive potentials: (a) $\Omega^* = -10$, (b) $\Omega^* = -50$, (c) $\Omega^* = -90$, and (d) $\Omega^* = -150$.

(figure 6) respectively. Also, the anticrossing and level repulsion appear clearly for the states around $m = -50$ in the energy dispersion. This interesting feature can be explained as follows. For the present geometry in the absence of the potential the dependence of the radial wavefunction on the distance takes the form $\sim R_n(\rho - \rho_m)$ where the centre of the wavefunction is $\rho_m = \sqrt{2\,|m|}r_B$ and R_n is the nth eigenfunction of a one-dimensional harmonic oscillator [29]. And, for $m = -50$ it is estimated that the radius $\rho_m = 10\,r_B$. Also, we have chosen the location of the delta potential to be at $\rho_p = 10\,r_B$ for the present calculation. Thus, those states near $m = -50$ are mostly influenced by the presence of the delta potential. The anticrossings in the energy spectrum become sharper for bigger $|\Omega^*|$. In figure 5 it is seen that levels which satisfy $|m + 50| \gg 0$ are almost unaffected by the δ-potential. In addition, we have seen that all states with positive magnetic quantum numbers are also unaffected by the δ-potential. However, as is seen from figure 6 for a large negative Ω^*, levels with $n = 0$ are pushed downward around $m = -50$, and consequently interaction with the states with $n \neq 0$ takes place at larger negative m. Also, differently from the case for the repulsive interaction, energies of the levels with positive m for $n = 0$ at strong enough $|\Omega^*|$ lose their unperturbed values, too. Increasing $|\Omega^*|$ further sweeps away energies of states with $n = 0$ for all m from values of the unperturbed magnetic field in figure 6(d). In the limit $\Omega^* \to -\infty$ it is seen that the energy eigenvalues of the states with $n = 0$ behave for all m as

$$E^* \sim -a + b\left(m + \frac{1}{2}r_p^2\right)^2 \tag{26}$$

where a and b are positive constants, which represents a quantum ring problem with rigidly bounded electrons subjected to a magnetic flux $\phi = \frac{1}{2}r_p^2$ [8]. Also, the energies of the states with $n \geqslant 1$ tend to usual Landau levels, equation (24), replacing n by $n - 1$ for large negative and all positive m.

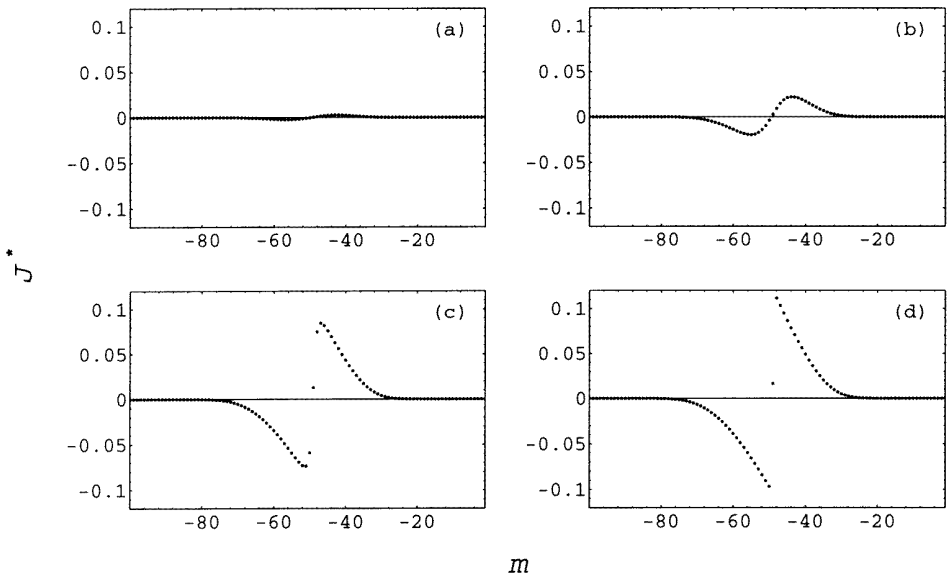

Figure 7. Currents J^* as a function of the magnetic index m for states with $n = 0$; the values of Ω^* in each part of the figure correspond to those from figure 5.

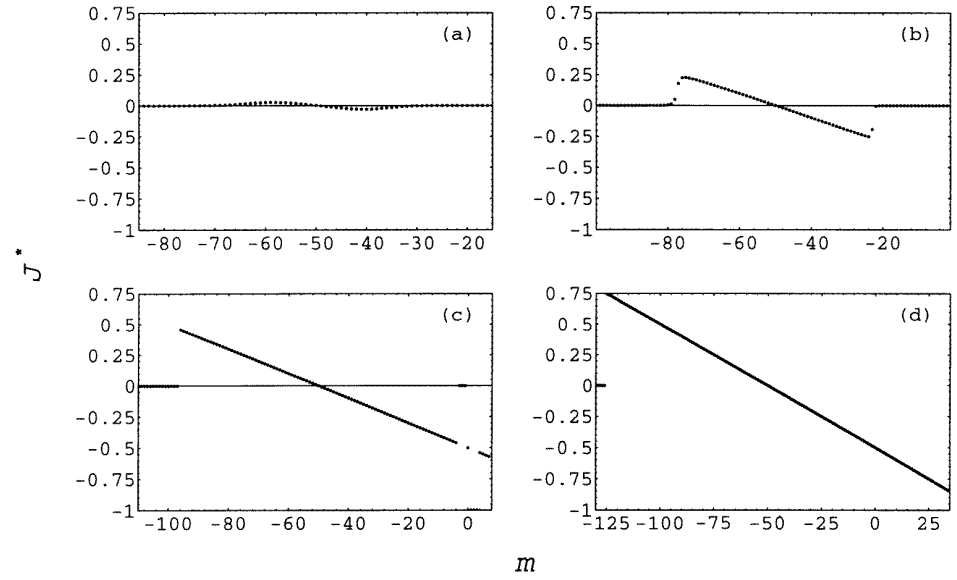

Figure 8. As figure 7; the values of Ω^* in each part of the figure correspond to those from figure 6.

In order to provide an insight into the transport problem the associated azimuthal currents with those states with $n = 0$ in figures 5 and 6 are depicted in figures 7 and 8 respectively,

where use has been made of the normalization

$$J^* = J \Big/ \left(\frac{e\omega_B}{2\pi}\right). \tag{27}$$

For the uniform magnetic field without any electrostatic potential, the current carried by the energy level with quantum numbers n and m is specified to be

$$J^* = \begin{cases} 0 & m < 0 \\ -\dfrac{1}{2} & m = 0 \\ -1 & m > 0 \end{cases} \tag{28}$$

which is independent of the radial quantum number n. The δ-potential introduced into the uniform magnetic fields leads to deviations of the currents from equation (28). The currents shown in figures 7 and 8 also follow from behaviour of the energy derivative with respect to the magnetic quantum number [29]

$$J^* = -\frac{e}{h}\frac{\partial E}{\partial m}. \tag{29}$$

For example, for a small positive opacity, the energy does not change appreciably with m (figure 5(a)) and the resulting currents are also small as would be expected from equation (29) (figure 7(a)). Increasing positive Ω^* results in larger deviations of the energy and consequently current compared to the uniform field results. As we mentioned before, states with $m = -50$ have a special meaning for the parameters chosen. For instance, the anticrossing between states with $n = 0$ and states with $n = 1$ occurs at this level of $m = -50$. And, the energy spectrum is symmetric about this level and its slope becomes discontinuous at large Ω^*. Consequently, an abrupt change is seen in the current, of which the behaviour becomes more evident for stronger Ω^*. Physically, levels with $|m| < 50$ for negative m correspond to the edge states located inside the ring potential and levels with $m < -50$ are the edge states outside the ring. Because of this, they carry opposite currents as is clearly seen from figure 7.

Currents carried by the states with $n = 0$ are plotted in figure 8 for negative opacity. Again, it is seen that a larger value of opacity causes more deviation of current from the values of equation (28). In this case the current vanishes identically for the state with $m = -50$, which can be understood as a consequence of equation (29). As in the case of a repulsive potential, the drastic changes of J^* occur at the anticrossing points. Comparing figures 7 and 8, one notices that the sign of the current for $\Omega^* < 0$ is opposite compared to that for positive potential. It is worthwhile to note also that for strong enough negative Ω^*, i.e. when the energy depends on m quadratically (see equation (26)), the corresponding current J^* is a linear function of the magnetic quantum number.

We have also seen that the currents carried by the states with $n > 0$ behave similarly: the anticrossing with adjacent levels gives rise to an interesting change in the current. Thus, it is confirmed that the anticrossings in the energy spectrum are important in determining transport properties of quantum systems in magnetic fields.

In conclusion, we have investigated the electronic and transport properties of a semiconductor microstructure modelled by a cylindrical δ-potential for various configurations of applied magnetic fields. It has been manifested that the results depend crucially on the distribution of magnetic fields and strength of the potential. Introduction of the electrostatic delta potential in uniform magnetic fields gives rise to the anticrossings and repulsions of the levels in the single-particle energy spectrum, which in turn results in the drastic change in the associated currents. Under limiting situations the previously known

results for the quantum ring and quantum disk have been recovered. The net equilibrium persistent current would be determined by summing all contributions from the energy levels weighted by the thermal distribution function in the usual manner. In the present work we have restricted our interest to the detailed analysis of the quantum currents carried by single-particle states.

Finally, we want to point out that the possibility of electron leakage outside the ring leads to the coupling between states of coaxial cylinders with different radii, which may give rise to some interesting new phenomena. By increasing the number of potentials one may devise a cylindrical superlattice. However, this is a subject for another special consideration in future work.

Acknowledgment

This work was supported by the Ministry of Education of Korea through the Basic Sciences Research Institutes at Chonnam National University (Grant No BSRI-95-2431).

References

[1] Park D K 1995 *J. Math. Phys.* **36** 5453
[2] Olendski O 1995 *J. Phys.: Condens. Matter* **7** 5067
[3] Johnson E A, MacKinnon A and Geobel C J 1987 *J. Phys. C: Solid State Phys.* **20** L521
[4] Ferreyra J M and Proetto C R 1994 *J. Phys.: Condens. Matter* **6** 6623
[5] Maan J C 1987 *Festkörperprobleme (Advances in Solid State Physics)* vol 27 (Braunschweig: Vieweg) p 137
[6] Aharonov Y and Bohm D 1959 *Phys. Rev.* **115** 485
[7] Magni C and Valz-Griz F 1995 *J. Math. Phys.* **36** 177
[8] Cheung H-F, Gefen Y, Riedel E K and Shih W-H 1988 *Phys. Rev.* B **37** 6050
[9] Cheung H-F, Riedel E K and Gefen Y 1989 *Phys. Rev. Lett.* **67** 3578
[10] Avishai Y, Hatsugai Y and Kohmoto M 1993 *Phys. Rev.* B **47** 9501
[11] Avishai Y and Kohmoto M 1993 *Phys. Rev. Lett.* **71** 279
[12] Vignale G 1995 *Phys. Rev.* B **51** 2612
[13] Kirczenow G 1995 *J. Phys.: Condens. Matter* **7** 2021
[14] Lévy L P, Dolan G, Dunsmuir J and Bouchiat H 1990 *Phys. Rev. Lett.* **64** 2074
[15] Chandrasekhar V, Webb R A, Brady M J, Ketchen M B, Gallagher W J and Kleinsasser A 1991 *Phys. Rev. Lett.* **67** 3578
[16] Mailly D, Chapelier C and Benoit A 1993 *Phys. Rev. Lett.* **70** 2020
[17] Büttiker M, Imry Y and Landauer R 1983 *Phys. Lett.* **96A** 365
[18] Avishai Y and Braverman G 1995 *Phys. Rev.* B **52** 12 135
[19] Wendler L, Fomin V M and Chaplik A V 1995 *Solid State Commun.* **96** 809
[20] Abramowitz M and Stegun I A (ed) 1964 *Handbook of Mathematical Functions* (New York: Dover)
[21] Flügge S 1971 *Practical Quantum Mechanics* vol 1 (Berlin: Springer)
[22] Landau L D and Lifshitz E M 1977 *Quantum Mechanics (Non-Relativistic Theory)* (New York: Pergamon)
[23] Foden C L, Leadbeater M L, Burroughes J H and Pepper M 1994 *J. Phys.: Condens. Matter* **6** L127
[24] Foden C L, Leadbeater M L and Pepper M 1995 *Phys. Rev.* B **52** R8646
[25] Carmona H A, Geim A K, Nogaret A, Main P C, Foster T J, Henini M, Beaumont S P and Blamire M G 1995 *Phys. Rev. Lett.* **74** 3009
[26] Ye P D, Weiss D, Gerhadts R P, Seeger M, von Klitzing K, Eberl K and Nickel H 1995 *Phys. Rev. Lett.* **74** 3013
[27] Leadbeater M L, Foden C L, Burke T M, Burroughes J H, Grimshaw M P, Ritchie D A, Wang L L and Pepper M 1995 *J. Phys.: Condens. Matter* **7** L307
[28] Geerinckx F, Peeters F M and Devreese J T 1990 *J. Appl. Phys.* **68** 3435
[29] Halperin B I 1982 *Phys. Rev.* B **25** 2185